Available online at www.sciencedirect.com
ScienceDirect
Tetrahedron
Tetrahedron 62 (2006) 10117–10122

# Exploiting the deprotonation mechanism for the design of ratiometric and colorimetric $Zn^{2+}$ fluorescent chemosensor with a large red-shift in emission

Zhaochao Xu,[a] Xuhong Qian,[a,b,c,*] Jingnan Cui[a,*] and Rong Zhang[a]

[a]*State Key Laboratory of Fine Chemicals, Dalian University of Technology, Dalian 116012, China*
[b]*Shanghai Key Laboratory of Chemical Biology, School of Pharmacy, East China University of Science and Technology, Shanghai 200237, China*
[c]*State Key Laboratory of Elemento-Organic Chemistry, Nankai University, China*

Received 22 May 2006; revised 11 August 2006; accepted 11 August 2006
Available online 7 September 2006

**Abstract**—The design, synthesis, and photophysical evaluation of a new naphthalimide-based fluorescent chemosensor, *N*-butyl-4-[di-(2-picolyl)amino]-5-(2-picolyl)amino-1,8-naphthalimide (**1**), were described for the detection of $Zn^{2+}$ in aqueous acetonitrile solution at pH 7.0. Probe **1** showed absorption at 451 nm and a strong fluorescence emission at 537 nm ($\Phi_F$=0.33). The capture of $Zn^{2+}$ by the receptor resulted in the deprotonation of the secondary amine conjugated to 1,8-naphthalimide so that the electron-donating ability of the N atom would be greatly enhanced; thus probe **1** showed a 56 nm red-shift in absorption (507 nm) and fluorescence spectra (593 nm, $\Phi_F$=0.14), respectively, from which one could sense $Zn^{2+}$ ratiometrically and colorimetrically. The deprotonated complex, [(**1**-H)/Zn]$^+$, was calculated at *m*/*z* 619.1800 and measured at *m*/*z* 618.9890. In contrast to these results, the emission of **1** was thoroughly quenched by $Cu^{2+}$, $Co^{2+}$, and $Ni^{2+}$. The addition of other metal ions such as $Li^+$, $Na^+$, $K^+$, $Mg^{2+}$, $Ca^{2+}$, $Fe^{3+}$, $Mn^{2+}$, $Al^{3+}$, $Cd^{2+}$, $Hg^{2+}$, $Ag^+$, and $Pb^{2+}$ produced a nominal change in the optical properties of **1** due to their low affinity to probe **1**. This means that probe **1** has a very high fluorescent imaging selectivity to $Zn^{2+}$ among metal ions.


## 1. Introduction

Chemosensors that convert molecular recognition into highly sensitive and easily detected signals have been actively investigated in recent years. A ratiometric and colorimetric fluorescent probes combine the sensitivity of fluorescence with the convenience and aesthetic appeal of a colorimetric assay.[1] In particular, ratiometric measurements have the important features that they permit signal rationing, and thus increase the dynamic range and provide built-in correction for environmental effects.[2]

The design of fluorescent probes for $Zn^{2+}$ is actively investigated,[3] as this metal ion is a critical trace element, playing significant roles in biological processes such as regulators of enzymes,[4] structural cofactors in metalloproteins, neural signal transmission,[5] and gene expression.[6] It is also known that a disorder of zinc metabolism is closely associated with many severe neurological diseases such as Alzheimer's disease (AD), amyotrophic lateral sclerosis (ALS), Guam ALS-Parkinsonism dementia, Parkinson's disease, hypoxia-ischemia, and epilepsy.[7] However, up to now, most of the $Zn^{2+}$ fluorescent probes are intensity-responsive based on PET quenching mechanism.[8] Only a few ratiometric and colorimetric fluorescent probes for $Zn^{2+}$ have been found in the literature. And still many efforts for a $Zn^{2+}$ fluorescent probe should be made among the issues, such as easy synthesis, visible light excitation, large red-shift in emission for $Zn^{2+}$ sensing, and no pH interference in the physiological pH range.

To carry out ratiometric measurements of $Zn^{2+}$ and get quantitative readouts, various mechanisms, which can cause a large shift in emission or excitation spectra have been introduced into $Zn^{2+}$ sensors such as excimer,[9] FRET,[10] ICT,[11] ESIPT,[12] two fluorophore approach,[13] conformational restriction,[14] time-resolved fluorescence techniques,[15] and self-assembly strategy.[16] Herein, we represent another new mechanism to design a ratiometric fluorescent probe for $Zn^{2+}$ based on deprotonation mechanism.

The secondary amines conjugated to 1,8-naphthalimide could be deprotonated by Cu(II)[1c] or $F^-$,[17] and as a result, large red shifts in both absorption and fluorescence spectra were obtained, from which one could sense $Cu^{2+}$ or $F^-$ colorimetrically and ratiometrically. In addition, the

*Keywords*: Ratiometric; $Zn^{2+}$ Fluorescent chemosensor; Naphthalimide; Deprotonation.
* Corresponding authors. Tel./fax: +86 411 83673488 (X.Q.); e-mail addresses: xhqian@ecust.edu.cn; jncui@chem.dlut.edu.cn

0040–4020/$ - see front matter © 2006 Elsevier Ltd. All rights reserved.
doi:10.1016/j.tet.2006.08.050

deprotonation of NH in amide or thiourea was believed to be the basis of $F^-$ sensing in recent research.[18] Based on the same deprotonation mechanism, which should not be a privilege confined to $Cu^{2+}$ or $F^-$, we introduced the well-known $Zn^{2+}$ receptor tris(2-pyridylmethyl)-amine (TPA) into 1,8-naphthalimide fluorophore and easily obtained fluorescent probe **1**, *N*-butyl-4-[di-(2-picolyl)amino]-5-(2-picolyl)amino-1,8-naphthalimide. The capture of $Zn^{2+}$ by the receptor resulted in the deprotonation of the secondary amine of **1**, which caused the ratiometric UV and fluorescence changes.

## 2. Results and discussions

### 2.1. Synthesis

The synthesis of **1** is shown in Scheme 1. The intermediate, compound **5**, was synthesized from acenaphthene following a literature procedure.[19] Compound **6** was prepared in 40.2% yield by the condensation of **5** with butylamine and was subsequently converted into compound **7**, which we have reported as a ratiometric $Cu^{2+}$ fluorescent sensor,[1b] through reaction with 2-aminomethylpyridine. Probe **1** was easily synthesized by conjugating picolyl chloride and compound **7** in 56.5% yield.

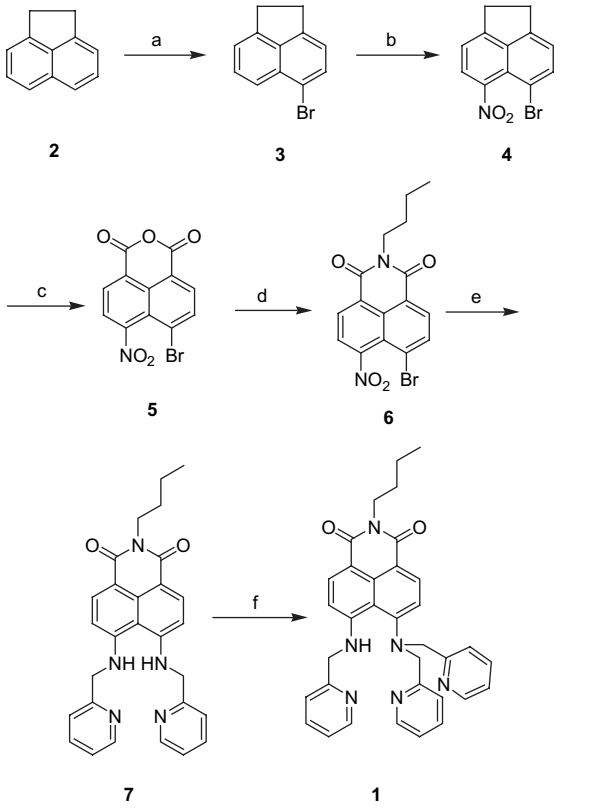


**Scheme 1**. Synthesis of **1**. (a) NBS, DMF, room temperature, 82.4%; (b) fuming $HNO_3$, AcOH, 10–15 °C, 53.1%; (c) $Na_2Cr_2O_7 \cdot 2H_2O$, AcOH, reflux, 51.7%; (d) $n$-$C_4H_9NH_2$, $C_2H_5OH$, reflux, 40.2%; (e) 2-aminomethylpyridine, $CH_3OC_2H_4OH$, $CH_3CN$, reflux, 85%; (f) picolyl chloride, $CH_3CN$, $K_2CO_3$, $N_2$, reflux, 56.5%.

### 2.2. ESIMS analysis

Probe **1** showed absorption at 451 nm and a strong fluorescence emission at 537 nm in acetonitrile–water (80:20)

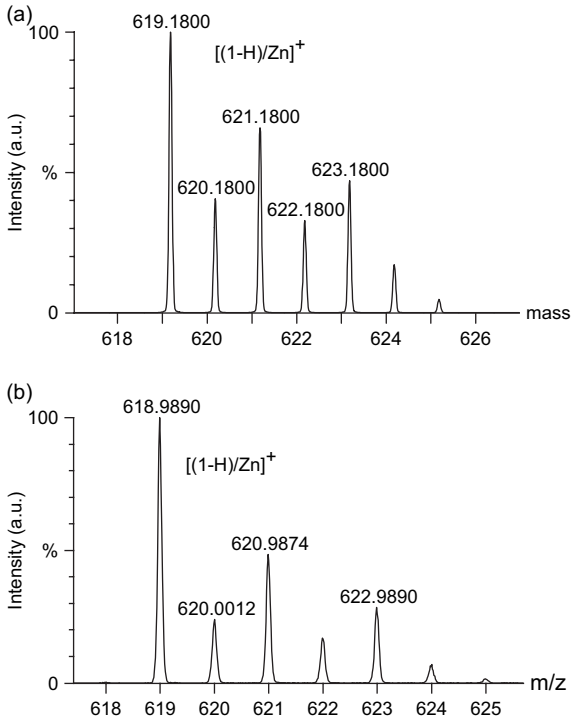


**Figure 1**. Electrospray mass spectrum of **1**-Zn sample in acetonitrile–water (80:20) solution at pH 7.0 maintained with HEPES buffer (50 mM). [**1**]=10 μM, [$Zn^{2+}$]=30 μM. (a) The calculated pattern of the most abundant complex [(**1**-H)/Zn]$^+$, $C_{34}H_{31}N_6O_2Zn$, $m/z$=619.1800. (b) The measured pattern of the most abundant complex [(**1**-H)/Zn]$^+$, $C_{34}H_{31}N_6O_2Zn$, $m/z$=618.9890.

solution. The capture of $Zn^{2+}$ by the receptor resulted in the deprotonation of the secondary amine so that the electron-donating ability of the N atom conjugated to the naphthalene ring would be greatly enhanced; thus probe **1** showed large red shifts in absorption and fluorescence spectra. The ESIMS analysis revealed single-charged complex [(**1**-H)/Zn]$^+$ that is formed due to the interaction of **1** with 1 equiv of $Zn^{2+}$ (Fig. 1). The [(**1**-H)/Zn]$^+$ complex was calculated at $m/z$ 619.1800 and measured at $m/z$ 618.9890. This indicated the formation of a **1**/$Zn^{2+}$ adduct of 1:1 stoichiometry.

### 2.3. The effect of pH

The influence of pH on the fluorescence of **1** was first determined by fluorescence titration in acetonitrile–water (80:20) solution (Fig. 2). The fluorescence of **1** at 537 nm remained unaffected between pH 13 and 4.21, and then gradually decreased from pH 4.21 to 1.77; below pH 1.77, no change in fluorescence was observed, leading to a sigmoid curve. Its p$K_a$ value was 3.0. The fluorescence quenching was most likely caused by the photo-induced electron transfer (PET) from the fluorophore to protonated pyridine.[20] de Silva had found the similar phenomenon in the design of an 'off-on-off' fluorescent PET sensor.[21] The influence of pH on the deprotonation of **1** induced by $Zn^{2+}$ was then investigated by means of the absorption and fluorescence measurements for a solution of 1 equiv of **1** and 2 equiv of $Zn^{2+}$. When 2 equiv of $Zn^{2+}$ was added to an acidic solution of **1** (pH=2), the absorbance at 451 nm steadily decreased,

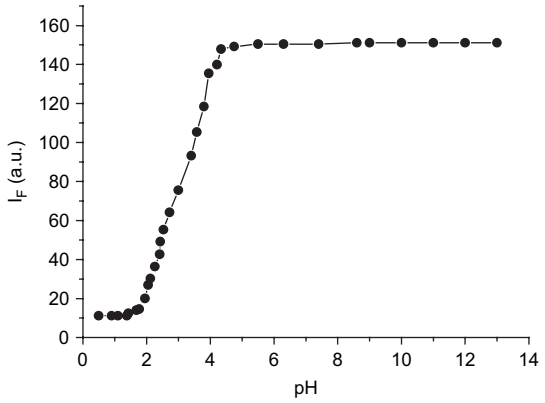


**Figure 2**. Influence of pH on the fluorescence of **1** in acetonitrile–water (80:20, v/v). Excitation wavelength is 470 nm. [**1**]=10 μM. The pH was modified by adding 75% $HClO_4$ or 10% $N^+(CH_3)_4OH^-$.

and a longer absorption band at 507 nm developed on titration with $N^+(CH_3)_4OH^-$ from pH 4.34 to 5.58 (Fig. 3a). The absorption *A* reached its limiting value between pH 5.58 and 8.3 after neutralization with the excess acid and on further addition of 1 equiv of base. The solution changed from primrose yellow to pink, in which [(**1**-H)/Zn]$^+$ became the dominant species. It was supposed that the three nitrogen atoms in pyridine rings and the deprotonated $N^-$ played the role of

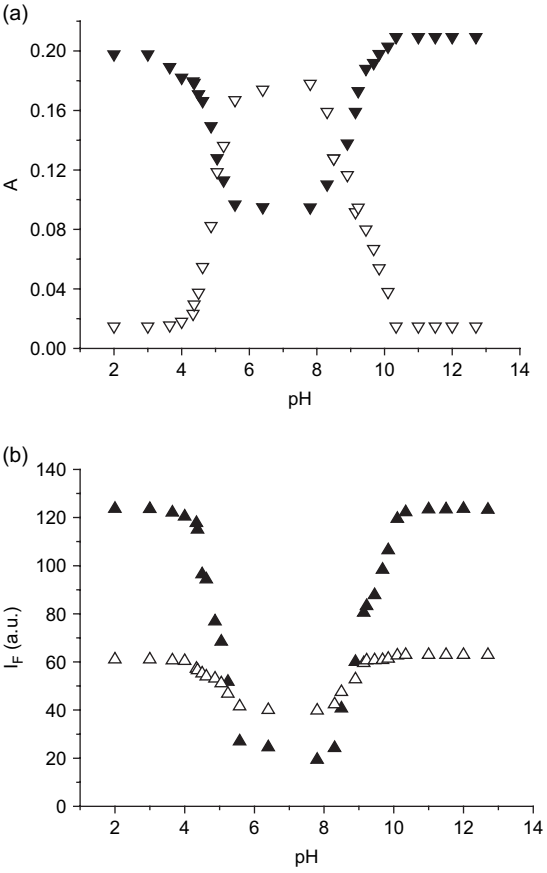


**Figure 3**. (a) Dependence of the absorbance of the band at 451 nm (▼) and 507 nm (▽) on pH for a solution of 1 equiv of **1** and 2 equiv of $Zn^{2+}$ in acetonitrile–water (80:20, v/v). [**1**]=10 μM. (b) Dependence of the fluorescence intensity of the band centered at 537 nm (▲) and 593 nm (△) on pH for a solution of 1 equiv of **1** and 2 equiv of $Zn^{2+}$ in acetonitrile–water (80:20, v/v). [**1**]=10 μM.

ligands to coordinate $Zn^{2+}$. On addition of more bases, the absorbance at 507 nm lessened and the absorption band at 451 nm restored from pH 8.3 to 10.34. This response may be due to the stronger complexation of $OH^-$ with $Zn^{2+}$ than the complexation of the deprotonated $N^-$ with $Zn^{2+}$. That means in strong basic conditions counter-reaction of deprotonation occurs, and $OH^-$ becomes one ligand instead of $N^-$. Simultaneously, a native emission band of **1** centered at 537 nm and a red-shifted fluorescence emission band centered at 593 nm attributed to [(**1**-H)/Zn]$^+$ were in the ascendant alternately according to the above three pH windows similar to absorption spectra (Fig. 3b). The four plots of *A* versus pH and $I_F$ versus pH all showed symmetrical bell-shaped curves centered at the same pH 7. Therefore, further and detailed studies were carried out in acetonitrile–water (80:20) solution at pH 7.0 maintained with HEPES buffer (50 mM). In our previous work,[1c] $OH^-$ played the role of base to cooperate with $Cu^{2+}$ to deprotonate the NH group conjugated to 1,8-naphthalimide, and then strong base would facilitate the deprotonation reaction much more. But in this case, $OH^-$ primarily played the role of ligand, which, on the contrary, speeded the reverse reaction of deprotonation. Thus these four plots in Figure 3 show symmetrical shapes.

### 2.4. Recognition of metal cations

The changes in absorption spectra during the $Zn^{2+}$ titration are shown in Figure 4. On addition of zinc ion to the solution of **1**, the absorption band at 451 nm decreased, and the other two bands at 309 and 507 nm occurred and increased prominently to their limiting values with isosbestic points at 382 and 470 nm, respectively. The emission spectra of **1** and its fluorescence titration with $Zn^{2+}$ are displayed in Figure 5. When $Zn^{2+}$ was added to the solution of **1**, a significant decrease in the 537 nm emission ($\Phi_F$=0.33) and a large red-shifted emission band centered at 593 nm ($\Delta E_{em}$=56 nm, $\Phi_F$=0.14) were observed with a clear isoemissive point at 630 nm. The binding constant was calculated to be $6.76\times10^5$ using the method reported in our previous work.[1b] The absorption and fluorescence spectra of **1** titrated with $Zn^{2+}$, after adding 0.1 equiv of $Zn^{2+}$ to the solution of **1** every time, were recorded in less than 30 s. If the interval was prolonged to 1 h, then the solution of **1** with 1 equiv of $Zn^{2+}$

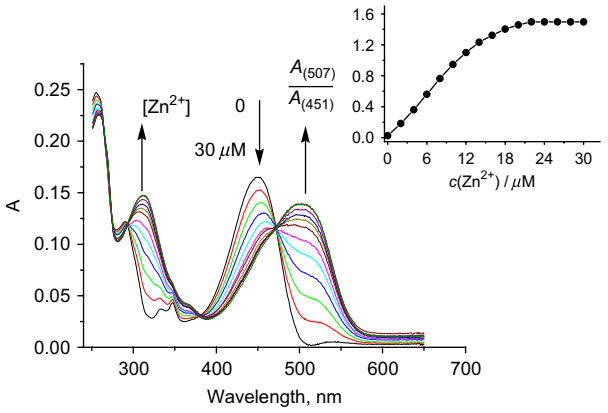


**Figure 4**. Dependence of the UV–vis absorption spectra of **1** on the concentration of $Zn^{2+}$ in acetonitrile–water (80:20) solution at pH 7.0 maintained with HEPES buffer (50 mM). [**1**]=10 μM, [$Zn^{2+}$]=0–30 μM. Inset: ratiometric calibration curve $A_{507}/A_{451}$ as a function of $Zn^{2+}$ concentration.

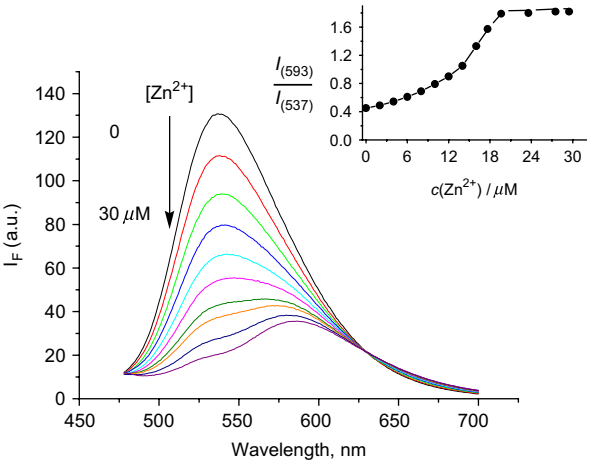


**Figure 5**. Fluorescent emission spectra of **1** in the presence of different concentrations of $Zn^{2+}$ in acetonitrile–water (80:20) solution at pH 7.0 maintained with HEPES buffer (50 mM). Excitation wavelength was 470 nm. [**1**]=10 μM, [$Zn^{2+}$]=0–30 μM. Inset: ratiometric calibration curve $I_{593}/I_{537}$ as a function of $Zn^{2+}$ concentration.

displayed the same absorption and fluorescence spectra as the solution of **1** with 2 equiv of $Zn^{2+}$. The insets in Figures 4 and 5 indicated that 2 equiv of $Zn^{2+}$ cooperating to react with 1 equiv of **1** could quickly reach the equilibrium in the formation of a (**1**-H)/$Zn^{2+}$ complex of 1:1 stoichiometry on comparison with 1 equiv of $Zn^{2+}$ with 1 equiv of **1**.

The titration of **1** with various metal ions was conducted to examine the selectivity. The addition of metal ions such as $Li^+$, $Na^+$, $K^+$, $Mg^{2+}$, $Ca^{2+}$, $Fe^{3+}$, $Mn^{2+}$, $Al^{3+}$, $Cd^{2+}$, $Hg^{2+}$, $Ag^+$, and $Pb^{2+}$ produced a nominal change in the optical properties of **1** due to their low affinity to probe **1**. The addition of $Cu^{2+}$, $Co^{2+}$, and $Ni^{2+}$ to the solution of **1** also can deprotonate probe **1** and change the solution color from primrose yellow to pink. However, in contrast with red-shifted emission induced by $Zn^{2+}$, the emission of **1** was thoroughly quenched by $Cu^{2+}$, $Co^{2+}$, and $Ni^{2+}$ (Fig. 6). This means that probe **1** has a very high fluorescent imaging selectivity to $Zn^{2+}$ (Fig. 7), although **1** does not show obvious binding discrimination among these four metal ions. This visible emission allows **1**+$Zn^{2+}$ to be readily distinguished by naked eye (Fig. 8), and sensor **1** thus combines

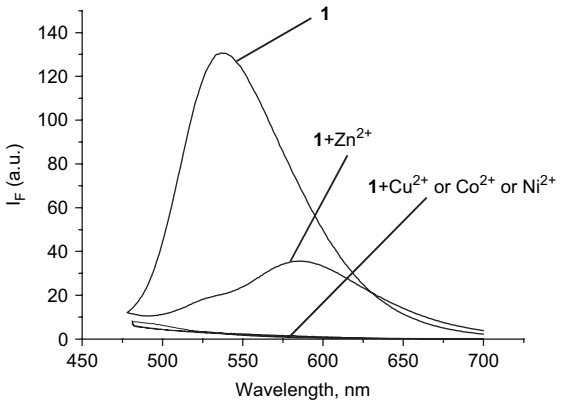


**Figure 6**. Fluorescent emission spectra of **1**, **1**+$Zn^{2+}$, and **1**+$Cu^{2+}$ (or $Co^{2+}$, or $Ni^{2+}$). [**1**]=10 μM, [$Zn^{2+}$]=[$Cu^{2+}$]=[$Co^{2+}$]=[$Ni^{2+}$]=30 μM.

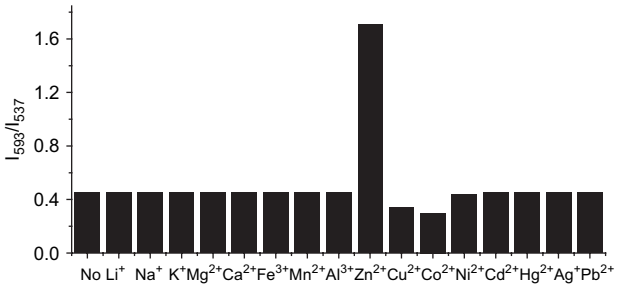


**Figure 7**. Fluorescence response of **1** to various metal ions in acetonitrile–water (80:20) solution at pH 7.0 maintained with HEPES buffer (50 mM). [**1**]=10 μM, and the concentration of each metal ion was 30 μM.

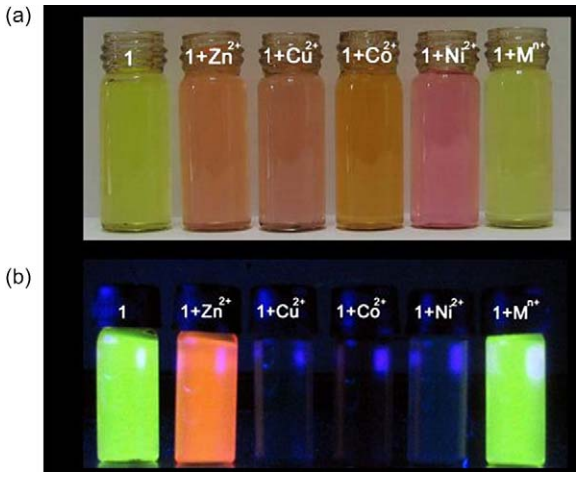


**Figure 8**. (a) Color change of compound **1** on addition of different metal ions. [**1**]=10 μM, [M]=30 μM. (b) Fluorescent emission observed from the solutions of **1** on addition of different metal ions. $M^{n+}$ represents other metal ions including $Li^+$, $Na^+$, $K^+$, $Mg^{2+}$, $Ca^{2+}$, $Fe^{3+}$, $Mn^{2+}$, $Al^{3+}$, $Cd^{2+}$, $Hg^{2+}$, $Ag^+$, and $Pb^{2+}$. Excitation wavelength is 365 nm emitted from a portable fluorescent lamp.

the sensitivity of fluorescence with the convenience and aesthetic appeal of a colorimetric assay.[2a]

Additionally, to explore the effects of anionic counterions on the sensing behavior of **1** to metal ions, fluorescence responses of **1** to perchlorate, chloride, and nitrate salts with different cations were examined. The results were similar to that shown in Figures 4 and 5. There were no obvious changes in the fluorescence responses of **1** to $Zn(ClO_4)_2$, $ZnCl_2$, and $Zn(NO_3)_2$.

## 3. Conclusion

We have demonstrated that probe **1** displayed a colorimetric response with a large red-shift emission that was useful for the easy detection of $Zn^{2+}$. The change in solution color from primrose yellow to pink and the red-shifted fluorescence spectra from green to red were attributed to the deprotonation of the secondary amine conjugated to the naphthalene ring. Probe **1** for $Zn^{2+}$ was developed from our former sensor[1b] for $Cu^{2+}$ on the base of the same deprotonation mechanism. With the improvement of selectivity for HTM ion receptors, we believe that this design strategy would help to extend the development of ratiometric fluorescent probes for other HTM ions.

## 4. Experimental

### 4.1. General

All the solvents were of analytic grade and used as received. The solutions of metal ions were prepared from $LiClO_4 \cdot 3H_2O$, $NaClO_4$, $KClO_4$, $MgCl_2 \cdot 6H_2O$, $CaCl_2$, $Fe(NO_3)_3$, $Mn(ClO_4)_2 \cdot 6H_2O$, $Al(ClO_4)_3$, $CoCl_2 \cdot 6H_2O$, $NiCl_2 \cdot 6H_2O$, $ZnCl_2$, $CdCl_2 \cdot 2½H_2O$, $CuCl_2 \cdot 2H_2O$, $HgCl_2$, $AgNO_3$, $Pb(NO_3)_2$, respectively, and were dissolved in distilled water. $^1H$ NMR were measured on a Bruker AV-400 spectrometer with chemical shifts reported as parts per million (in $CDCl_3$/DMSO-$d_6$, TMS as internal standard). Mass spectra were measured on an HP 1100 LC-MS spectrometer. Melting points were determined by an X-6 micro-melting point apparatus and are uncorrected. IR spectra were recorded on a Nicolet Nexus 770 spectrometer. All pH measurements were made with a Sartorius basic pH-Meter PB-20. Fluorescence spectra were determined on a Hitachi F-4500. Absorption spectra were determined on a PGENERAL TU-1901 UV–vis spectrophotometer. The fluorescence quantum yields ($\Phi_F$) were estimated with *N*-butyl-4-butylamino-1,8-naphthalimide in absolute ethanol as a standard ($\Phi_F$=0.81).[22]

### 4.2. Synthesis

**4.2.1. *N*-Butyl-4-bromo-5-nitro-1,8-naphthalimide (6).** To a solution of 200 mg (0.62 mmol) 4-bromo-5-nitro-1,8-naphthalic anhydride (**5**) in 20 mL ethanol was added dropwise 45 mg (0.62 mmol) butylamine in 6 mL ethanol. The mixture was then heated at reflux for 40 min and monitored by TLC. After the reaction was completed, the solvent was removed under reduced pressure. The crude product was then purified by column chromatography ($SiO_2$, $CHCl_3$) to give (**6**) as a white solid in 40.2% yield (94 mg). Mp: 175.8–176.2 °C. $^1H$ NMR ($CDCl_3$, 400 MHz) $\delta$ 0.99 (t, $J$=7.2 Hz, 3H), 1.42–1.48 (m, $J$=7.2 Hz, 2H), 1.68–1.74 (m, $J$=7.2 Hz, 2H), 4.18 (t, $J$=7.2 Hz, 2H), 7.93 (d, $J$=8.0 Hz, 1H), 8.21 (d, $J$=8.0 Hz, 1H), 8.51 (d, $J$=8.0 Hz, 1H), 8.71 (d, $J$=8.0 Hz, 1H). $^{13}C$ NMR ($CDCl_3$, 100 MHz) $\delta$ 13.95, 20.49, 30.21, 40.92, 122.69, 123.72, 124.26, 125.99, 131.37, 132.49, 136.14, 162.21, 162.98. IR (KBr, $cm^{-1}$): 3057, 2963, 2935, 2912, 2860, 1706, 1568, 1541, 1230, 658, 586. HRMS (EI) calcd for $C_{16}H_{13}BrN_2O_4$ [$M^+$]: 376.0059, found: 376.0075.

**4.2.2. *N*-Butyl-4,5-di[(2-picolyl)amino]-1,8-naphthalimide (7).** 2-(Aminomethyl)pyridine (0.3 mL, 2.89 mmol) was added dropwise to a solution of 53 mg (0.141 mmol) *N*-butyl-4-bromo-5-nitro-1,8-naphthalimide (**6**) in 1.0 mL 2-methoxyethanol, and then the mixture was heated to reflux for 3 h and monitored by TLC. After the reaction was completed, the solution was cooled at room temperature to give yellow needle crystals. The product was filtered off, washed with 2-methoxyethanol, and then dried in air. The product was then purified by column chromatography ($SiO_2$, $CH_2Cl_2$/EtOAC, 2:1, v/v) to give **7** as a yellow powder in 85% yield (56 mg). Mp: 179.5–179.9 °C. $^1H$ NMR ($CDCl_3$, 400 MHz) $\delta$ 0.95 (t, $J$=7.6 Hz, 3H), 1.41–1.47 (m, $J$=7.6 Hz, 2H), 1.66–1.72 (m, $J$=7.6 Hz, 2H), 4.14 (t, $J$=7.6 Hz, 2H), 4.66 (s, 4H), 6.78 (d, $J$=8.4 Hz, 2H), 7.19 (t, $J$=7.2 Hz, 2H), 7.40 (d, $J$=7.6 Hz, 2H), 7.62 (S, N–H), 7.69 (t, $J$=7.2 Hz, 2H), 8.32 (d, $J$=8.4 Hz, 2H), 8.42 (d, $J$=8.4 Hz, 2H). $^{13}C$ NMR ($CDCl_3$, 100 MHz) $\delta$ 14.09, 20.65, 30.55, 39.97, 49.36, 105.98, 107.24, 112.38, 122.16, 122.77, 133.87, 137.24, 147.75, 149.06, 151.93, 156.31, 164.83. IR (KBr, $cm^{-1}$): 3328, 3043, 2953, 2869, 1673, 1633, 1592, 1541, 1508, 1310, 996. HRMS (ESI) calcd for $C_{28}H_{28}N_5O_2$ [$MH^+$]: 466.2243, found: 466.2247.

**4.2.3. *N*-Butyl-4-[di-(2-picolyl)amino]-5-(2-picolyl)-amino-1,8-naphthalimide (1).** To a solution of 200 mg (0.43 mmol) *N*-butyl-4,5-di[(pyridin-2-ylmethyl)amino]-1,8-naphthalimide (**7**) in 5 mL dry acetonitrile were added 57 mg (0.46 mmol) picolyl chloride and 150 mg $K_2CO_3$. The mixture was then heated at reflux for 2 h under nitrogen and monitored by TLC. After the reaction was completed, the solvent was removed under reduced pressure. The crude product was then purified by alumina column chromatography ($CH_2Cl_2$:MeOH=100:5) to give **1** as a yellow solid in 56.5% yield (135 mg). Mp: 133.6–134.9 °C. $^1H$ NMR ($CDCl_3$, 400 MHz) $\delta$ 0.95 (t, $J$=7.2 Hz, 3H), 1.39–1.45 (m, $J$=7.2 Hz, 2H), 1.64–1.70 (m, $J$=7.2 Hz, 2H), 4.12 (t, $J$=7.2 Hz, 2H), 4.54 (s, 4H), 4.93 (s, 2H), 6.61 (d, $J$=8.4 Hz, 1H), 7.09 (d, $J$=8.0 Hz, 2H), 7.12–7.17 (m, 3H), 7.22 (t, $J$=7.2 Hz, 1H), 7.36 (d, $J$=8.0 Hz, 1H), 7.55 (t, $J$=7.6 Hz, 2H), 7.61 (d, $J$=7.6 Hz, 1H), 8.35 (d, $J$=8.4 Hz, 1H), 8.38 (d, $J$=8.4 Hz, 1H), 8.50 (d, $J$=4.8 Hz, 2H), 8.62 (d, $J$=4.4 Hz, 1H), 11.58 (s, 1H, NH). $^{13}C$ NMR ($CDCl_3$, 100 MHz) $\delta$ 14.08, 20.63, 30.46, 40.01, 49.24, 59.64, 105.39, 109.17, 115.65, 119.24, 119.65, 121.16, 122.46, 122.78, 123.85, 131.52, 132.88, 134.75, 136.77, 137.03, 149.65, 152.65, 154.56, 156.33, 158.33, 164.48, 164.75. IR (KBr, $cm^{-1}$): 3435, 3182, 2954, 2869, 1679, 1638, 1578, 1541, 1433, 1397, 1356, 1317, 1240, 817, 750, 612. HRMS (ESI) calcd for $C_{34}H_{32}N_6O_2$ [$MH^+$]: 557.2665, found: 557.2662.


## Acknowledgements

Financial support by the National Key Project for Basic Research (2003CB114400) and under the auspices of National Natural Science Foundation of China is greatly appreciated.


## Supplementary data

Spectroscopic data of **1** upon titration with $Cu^{2+}$, $Co^{2+}$, and $Ni^{2+}$. Supplementary data associated with this article can be found in the online version, at doi:10.1016/j.tet.2006.08.050.

## References and notes


1. (a) Kubo, Y.; Yamamoto, M.; Ikeda, M.; Takeuchi, M.; Shinkai, S.; Yamaguchi, S.; Tamao, K. *Angew. Chem., Int. Ed.* **2003**, *42*, 2036–2040; (b) Xu, Z.; Xiao, Y.; Qian, X.; Cui, J.; Cui, D. *Org. Lett.* **2005**, *7*, 889–892; (c) Xu, Z.; Qian, X.; Cui, J. *Org. Lett.* **2005**, *7*, 3029–3032.
2. (a) Mello, J. V.; Finney, N. S. *Angew. Chem., Int. Ed.* **2001**, *40*, 1536–1538; (b) Takakusa, H.; Kikuchi, K.; Urano, Y.; Sakamoto, S.; Yamaguchi, K.; Nagano, T. *J. Am. Chem. Soc.* **2002**, *124*, 1653–1657; (c) Choi, K.; Hamilton, A. D. *Angew. Chem., Int. Ed.* **2001**, *40*, 3912–3915.

3. (a) Gee, K. R.; Zhou, Z.; Qian, W.; Kennedy, R. *J. Am. Chem. Soc.* **2002**, *124*, 776–778; (b) Gunnlaugsson, T.; Lee, T. C.; Parkesh, R. *Org. Biomol. Chem.* **2003**, *1*, 3265–3267; (c) Burdette, S. C.; Frederickson, C. J.; Bu, W.; Lippard, S. J. *J. Am. Chem. Soc.* **2003**, *125*, 1778–1787; (d) Komatsu, K.; Kikuchi, K.; Kojima, H.; Urano, Y.; Nagano, T. *J. Am. Chem. Soc.* **2005**, *127*, 10197–10204.
4. Berg, J. M.; Shi, Y. *Science* **1996**, *271*, 1081–1085.
5. Burdette, S. C.; Lippard, S. J. *Proc. Natl. Acad. Sci. U.S.A.* **2003**, *100*, 3605–3610.
6. Andrews, G. K. *Biometals* **2001**, *14*, 223–237.
7. Cuajungco, M. P.; Lees, G. J. *Neurobiol. Dis.* **1997**, *4*, 137–169.
8. (a) See Refs. 3a,b; (b) Burdette, S. C.; Frederickson, C. J.; Bu, W.; Lippard, S. J. *J. Am. Chem. Soc.* **2003**, *125*, 1778–1787; (c) Komatsu, K.; Kikuchi, K.; Kojima, H.; Urano, Y.; Nagano, T. *J. Am. Chem. Soc.* **2005**, *127*, 10197–10204.
9. Sclafani, J. A.; Maranto, M. T.; Sisk, T. M.; Arman, S. A. V. *Tetrahedron Lett.* **1996**, *37*, 2193–2196.
10. (a) Thompson, R. B.; Cramer, M. L.; Bozym, R. A.; Fierke, C. A. *J. Biomed. Opt.* **2002**, *7*, 555–560; (b) Bozym, R. A.; Thompson, R. B.; Stoddard, A. K.; Fierke, C. A. *ACS Chem. Biol.* **2006**, *1*, 103–111.
11. (a) Maruyama, S.; Kikuchi, K.; Hirano, T.; Urano, Y.; Nagano, T. *J. Am. Chem. Soc.* **2002**, *124*, 10650–10651; (b) Taki, M.; Wolford, J. L.; O'Halloran, T. V. *J. Am. Chem. Soc.* **2004**, *126*, 712–713; (c) Lim, N. C.; Schuster, J. V.; Porto, M. C.; Tanudra, M. A.; Yao, L.; Freake, H. C.; Bruckner, C. *Inorg. Chem.* **2005**, *44*, 2018–2030.
12. Henary, M. M.; Wu, Y.; Fahrni, C. J. *Chem.—Eur. J.* **2004**, *10*, 3015–3025.
13. Woodroofe, C. C.; Lippard, S. J. *J. Am. Chem. Soc.* **2003**, *125*, 11458–11459.
14. Ajayaghosh, A.; Carol, P.; Sreejith, S. *J. Am. Chem. Soc.* **2005**, *127*, 14962–14963.
15. Royzen, M.; Durandin, A.; Young, V. G.; Geacintov, N. E.; Canary, J. W. *J. Am. Chem. Soc.* **2006**, *128*, 3854–3855.
16. Wu, Z.; Zhang, Y.; Ma, J. S.; Yang, G. *Inorg. Chem.* **2006**, *45*, 3140–3142.
17. (a) Gunnlaugsson, T.; Kruger, P. E.; Lee, T. C.; Parkesh, R.; Pfeffer, F. M.; Hussey, G. M. *Tetrahedron Lett.* **2003**, *44*, 6575–6578; (b) Gunnlaugsson, T.; Kruger, P. E.; Jensen, P.; Pfeffer, F. M.; Hussey, G. M. *Tetrahedron Lett.* **2003**, *44*, 8909–8913.
18. Boiocchi, M.; Boca, L. D.; Gómez, D. E.; Fabbrizzi, L.; Licchelli, M.; Monzani, E. *J. Am. Chem. Soc.* **2004**, *126*, 16507–16514.
19. Peters, A. T.; Behesti, Y. S. S. *J. Soc. Dyers Colour* **1989**, *105*, 29–35.
20. (a) de Silva, A. P.; Nimal Gunaratne, H. Q.; Lynch, P. L. M. *J. Chem. Soc., Perkin Trans. 2* **1995**, 685–690; (b) Saeva, F. D. *J. Photochem. Photobiol., A: Chem.* **1994**, *78*, 201–204.
21. de Silva, A. P.; Nimal Gunaratne, H. Q.; McCoy, C. P. *Chem. Commun.* **1996**, 2399–2400.
22. Guo, X.; Qian, X.; Jia, L. *J. Am. Chem. Soc.* **2004**, *126*, 2272–2273.